DATA EVALUATION FOR DEPTH CALIBRATION OF A CUSTOMARY PMD RANGE IMAGING SENSOR CONSIDERING OBJECTS WITH DIFFERENT ALBEDO

Jochen Radmer
Institut für Werkzeugmaschinen und Fabrikbetrieb (IWF), Technische Universität Berlin, Berlin, Germany

Alexander Sabov and Jörg Krüger
Institut für Produktionsanlagen und Konstruktionstechnik (IPK), Fraunhofer Gesellschaft, Berlin, Germany

Keywords: Range Imaging Camera, Photo Mixer Device (PMD), Depth Calibration, Albedo, Reflectance Properties.

Abstract: For various applications, such as object recognition or tracking and especially when the object is partly occluded or articulated, 3D information is crucial for the robustness of the application. A recently developed sensor to aquire distance information is based on the Photo Mixer Device *(PMD)* technique. This article presents an easy but accurate data acquisition method for data evaluation of a customary sensor. Data evaluation focuses on the detection of the over- and underexposured data under consideration of objects with two different albedos.

1 INTRODUCTION

Since we are living in a three-dimensional world, for various applications, such as object recognition or tracking, 3D information is crucial for the robustness of the application, especially when the object is partly occluded or articulated. Due to its significance, the field of depth data acquisition has attracted many researchers working on sensors or sensor systems respectively. A recently developed sensor is based on the Photo Mixer Device *(PMD)* technique which works on modulated, coherent infrared light using the Time of Flight *(ToF)* approach and rely on a technology that correlates reference and received signals directly on the chip. It was first mentioned by (Lange, 2000) and (Schwarte, 1999). This sensor provides direct depth information for a whole image, for which reason such sensors are called range imaging sensors. Additionally to the depth data the camera provides two other channels. One channel corresponds to the luminance of the scene and the other channel is the amplitude as it is described in section (Lange, 2000) and corresponds to the signal strength of the incoming signal. The PMD range imaging camera is shown in figure 1 with infrared LED matrices on both sides of the camera.

Figure 1: This figure shows the examined PMD Range Imaging Camera of model PMD [vision] 19k with the infrared LED matrices on both sides of the camera.

Since this sensor is based on a rather new technology, data evaluation and depth calibration has to be carried out for it. (Lindner and Kolb, 2006) did a lateral and depth calibration on a modified research sensor. In this work the non-linearity of the depth data was coped by a distance deviation plot. (Kahlmann et al., 2006) additionally considered the dependency on the integration time. But since the sensor emits light for *ToF* and is dependent on the amount of incident light, the integration time is not the only parameter affecting the depth measurement. It is just one parameter influencing the amount of incident light. The incident light can also vary with the infrared reflectance properties of the looked at object, the distance to it and the LEDs properties. Therefore the data evaluation for the depth calibration has to be car-

Radmer J., Sabov A. and Krüger J. (2008).
DATA EVALUATION FOR DEPTH CALIBRATION OF A CUSTOMARY PMD RANGE IMAGING SENSOR CONSIDERING OBJECTS WITH DIFFERENT ALBEDO.
In *Proceedings of the Third International Conference on Computer Vision Theory and Applications*, pages 169-173
DOI: 10.5220/0001076701690173

ried out considering the amount of incident light. In addition, in order to guarantee a certain exactitude of the data, over and underexposed data has to be identified. For this reason this paper focuses on data evaluation and improvement considering different reflectance properties in combination with the distance and the integration time for a customary sensor. On account of the fact that the reflectance properties of an object vary greatly with its material and orientation, the measurement will be simplified. Instead of the reflectivity we will rather consider different albedos. Albedo is a unitless measure indicative of an object's diffuse reflectance properties. Nevertheless, a comprehensive investigation has to be done for many reflectance properties so that this work can be seen as some starting point. Thus, the main contribution of this paper is the analysis of the data provided by the PMD range camera under consideration of objects with different albedos and to give method for distance measuring improvement.

The distance measuring methods used be the PMD range imaging camera is the Time of Flight *(ToF)* method. The article of (Lange, 2000) offers a detailed description of the functional way of the PMD range imaging camera. A short overview of the distance calculation can be found in (Sabov and Kruger, 2007).

The paper is structured as follows. First the data acquisition and data evaluation is described. The basic methods for the improvement of the data are given. Within section three results are presented and discussed and finally this article is concluded in section five.

2 DATA EVALUATION

2.1 Data Acquisition Method

For the data evaluation fixed targets were considered, a black and a white wall, with diffuse, Lambertian reflectance model like characteristics. We have selected a white and a black wall as objects because of their contrariness in their albedo.

The measuring setup for the data acquisition existed of the PMD range camera, two lasers to distance measuring instruments (range finder), a camera construction to arm the distance measuring instruments on the PMD range camera, two markers, a tripod and the object, the wall. The measurement range of the distance measuring instrument was $0.2m$ to $30m$ meter with an accuracy of $\pm 2.0mm$. Those range finders were aimed at the ends of the camera construction in parallel in the direction of the camera. With every

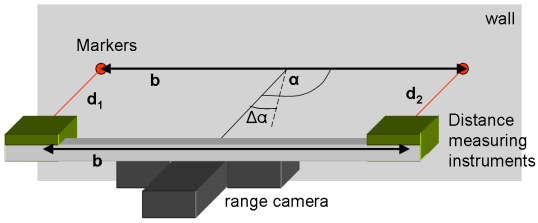

Figure 2: This figure shows the measurement setup as described in the text.

measurement the camera was aimed with both distance measuring instruments showing the same distance. The distance measured by both instruments was taken as the nominal distance to the object. In addition, the laser points of the distance measuring instruments were directed upon two marks on the wall to verify the parallelism of the distance measuring instruments. The base distance b between the marks on the wall as well as the distance between both range finders is identical. To guarantee the orientation of the camera also in vertical direction, the marks were appropriated by the same height like the range finders. The base distance b can be seen in the figure 2, which shows the whole measurement setup. The parallelism and the same distances measured by the instruments guaranteed the horizontal orientation α of the camera towards the wall to be perpendicular. This is done to reduce perspective influence on the measurement. Based on this measuring setup and with the base distance $b = 0.4m$ the maximum angle error $\Delta\alpha_{max}$ of the adjustment of the camera arises to $\Delta\alpha_{max} \approx 0.6°$ using the following equation:

$$\Delta\alpha_{max} = \arctan\frac{|\Delta d_1| + |\Delta d_2|}{b} = \arctan\frac{0.004m}{0.4m} \quad (1)$$

This assumes that the wall is plane and arming of the range finders was performed in a precise way. The maximum distance error Δd_{max} can be calculated regarding the direction of the distances with equation 2. The maximum Δd_{max} then arises to $\pm 2.0mm$.

$$\Delta d_{max} = \frac{\Delta d_1 + \Delta d_2}{2} \quad (2)$$

The measurement was carried out in different distances of the camera to the wall in intervals between the single measurements of $0.1m$. The measurement was applied about the whole measuring space of the camera. Ten measurements were carried out in every measuring distance and in each case the local neighborhood of the centre was captured to get more stable data. The centre was determined before by the determination of the intrinsic parameters. This lateral calibration was done using the method described

in (Bouguet, 1999). The measurements per measuring distance were performed for different integration times. The span of the used integration times reached from 500μs to 20000μs which were gone through in 500μs steps.
(Kahlmann et al., 2006) showed that the sensor 'SwissRanger' heats up self-induced and that this affects the captured data. This process stabilizes a few minutes after having started the data acquisition. To avoid these effects of self-induced heating, the data acquisition for the data evaluation was started after 20 minutes of sensor run-time.

Although the distance measurement accuracy vary over the sensor and every measuring point must be considered individually for improvement (Kahlmann et al., 2006), in this work only the central measuring points are considered, because the focus on the distance data improvement lies in relation for the integration time, the nominal distance and the albedo of the objects.

2.2 Distance Measurement, Amplitude and Object Albedo

In this section distance measuring results regarding integration time and nominal distance are considered. First it is looked at the measuring results without varying the albedo of the object. In figure 3 the deviation of the measured to the nominal distance for a white wall can be seen. The deviations are applied for integration time and nominal distance. As can be seen clearly, low integration times and high nominal distances result in erroneous distance measurements. In this connection must be mentioned that the low integration times which yield erroneous distance measuring values play only one very low role in the practical use of the sensor. The same can be ascertained for long integration times in combination with low nominal distances. Since distance measurements with under- and overexposure do not include any useful information, these distances have to be detected first before improving the distance data.

In the area in which the measured distances deviate only slightly from the nominal ones a periodical dependence of the distance offset can be ascertained to the nominal distance. This periodic error in the depth measurement agrees with mathematical predictions due to the shape of the correlation function of the reference and the received signals. Beside this periodical dependence the distance measuring error increases with an enlargement of the integration time. The error measured for different integration times tending downwards has a range of about 50mm up from 2m nominal distances. For closer distances

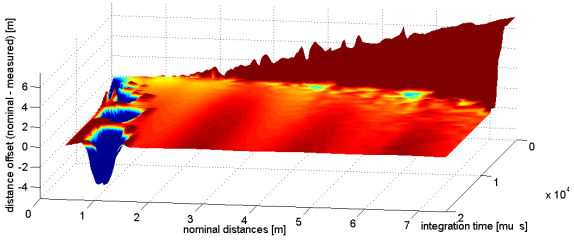

Figure 3: This figure shows the absolute deviation of nominal to measured distances in meter regarding the integration times in $\mu s 10^4$ and nominal distance in meter. A white wall with diffuse, Lambertian reflectance model like characteristics had been considered as object.

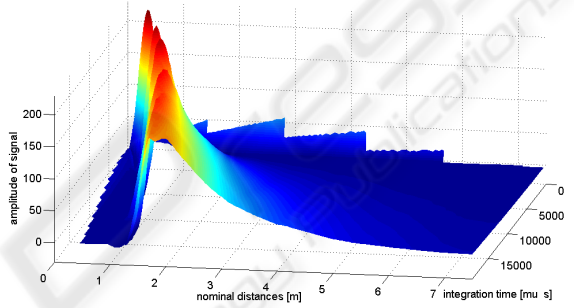

Figure 4: This figure shows the amplitude of the signal used for distance determination regarding the integration times in μs and nominal distance in meter. A white wall was used as object.

the error introduced by the near field effect caused by different *ToF* from the left and the right LED arrays dominates over the error introduced by the anharmonic signals. For these areas which can be described about integration time and nominal distance a correction can be achieved about Look-up-tables *(LUT)*. According to (Kahlmann et al., 2006) these LUT's have to contain an individual offset for each data point. A better knowledge of the received LED and the reference signal likely would provide a more robust basis for depth calibration. However, with the practical application of the sensor the nominal distance is unknown. Hence, we take into consideration for the detection of the useless distance values, in addition, the amplitude *Ampl*. In figure 4 the accompanying *Ampl* is shown. Likewise with regard to the integration time and the nominal distance. A connection can be noticed between distance measuring error and the accompanying *Ampl*. Through a simple threshold the underexposed data can be identified, when *Ampl* falls below a certain threshold.

The area in which on account of low nominal distance, high reflectance property and long integration time it comes to an overexposure cannot be detected simply about a threshold. In this case the standard

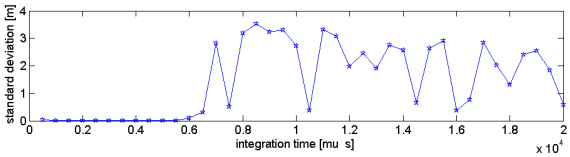

Figure 5: This figure shows the standard deviation in meter regarding the integration times in $\mu s 10^4$. A white wall was considered as object with a nominal distance of $0.9m$. It can be noticed that the standard deviation can be used for the detection of overexposure.

deviation of the distance is considered giving a direct quality measurement for the measured distances. Exemplary the standard deviation for the distance measurement at a nominal distance of $0.9m$ is shown in figure 5. It was computed out of ten measured distances. The nominal distance of $0.9m$ was selected because it yields correctable distance values at short integration times and arbitrary distance values at long ones, which are not correctable (cp. figure 3). Figure 5 shows that the standard deviation is high when an overexposure occurs and low instead. Therefore the standard deviation of measured distances can be used for the detection of overexposure. It can be seen that the standard deviation in spite of the very small number of ten samples being used for the calculation achieves a high discriminatory power. Comparable results can be achieved by calculating the standard deviation of the local neighborhood and therefore using a spatial instead of a temporal window. A spatiotemporal consideration is not necessary because of the high discriminatory power of one approach.

By the detection of over- and underexposure useless measured distances can be neglected. The remaining measured distances then can be corrected by a LUT, which is based upon the nominal to measured distance measurements.

In the following the measuring results are examined under consideration of a different albedo of the object. For measurements with a black wall as object the distance offset can be seen in figure 6. Of course these measurements also show areas with erroneous measured distances due to underexposure, since the albedo of a black wall is lower than the one of a white wall. The recently described method for the detection of measured distance in case of over- or underexposure show good results also with this object, when using the same global thresholds. The periodicity has the same period length over the nominal distance. This is due to the shape of the correlation function of the reference and the received signals, which does not change. But in comparison to the measurements with the white wall, a bigger distance offset can be

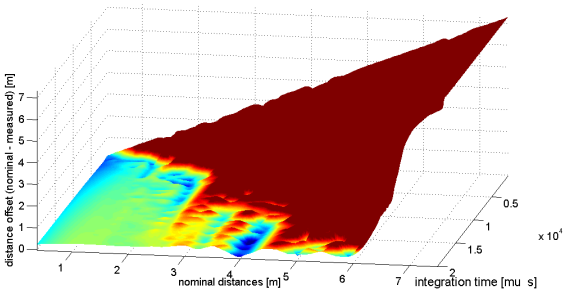

Figure 6: This figure shows the absolute deviation of nominal to measured distances in meter regarding the integration times in $\mu s 10^4$ and nominal distance in meter. A black wall was used as object.

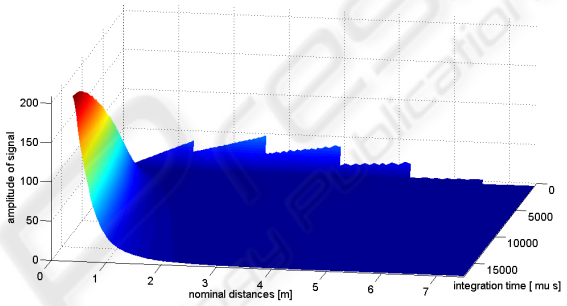

Figure 7: This figure shows the amplitude of the signal used for distance determination regarding the integration times in μs and nominal distance in meter. A black wall was used as object.

noticed. Therefore the albedo must be identified for the improvement of the distance measuring data.
Since the range camera works with a globally set integration time, the method for the improvement of the data needs to take into consideration the amount of incident light. That can be achieved by directly considering $Ampl$. Figure 7 shows $Ampl$ of the measurements with the black wall. Results for the identification of the albedo with a case-based measured distance improvement are presented in the next section.

3 RESULTS

In this section the results of the work are presented, meaning that the identification of the albedo with a case-based distance value improvement are presented for a black and white wall. In figure 8 is shown on the left side the distance offset in meter and on the right side the according amplitude $Ampl$ at central data points along a central column. The left side shows the black wall and the right side the white wall show-

ing a lower distance measuring error. The crossover between black and white can be seen clearly. The result after applying the LUT's for black and white on the distance measurement data is shown in figure 9 showing the distance offset in meter. It can be noticed that the distance offsets were decreased significantly from up to $0.3m$ down to about $0.02m$. The difference of the distance offset between the white and the black wall was nearly completely eliminated. At data points where the different albedo contact a bigger distance offset can be noticed. This is caused by the intermediate values for which no LUT exist.

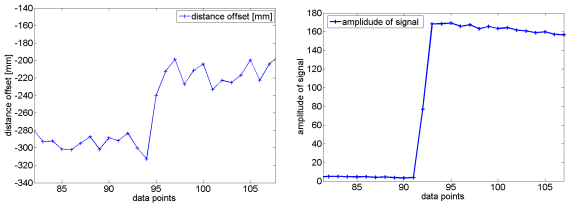

Figure 8: In the left figure the distance offset in meter and on the right side the according amplitude *Ampl* at central data points along a central column is shown. The crossover between the two albedos can be seen clearly.

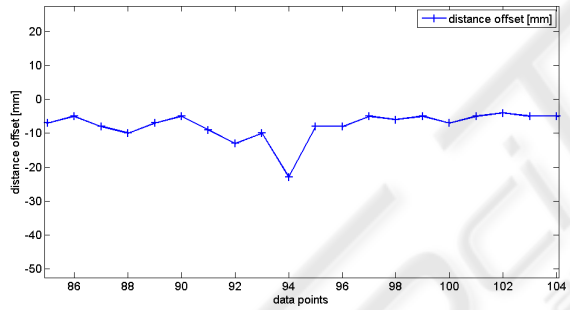

Figure 9: This figure shows the distance offset in meter after applying the LUT's for black and white on the distance measurement data. The distance offsets were decreased from up to $0.3m$ down to about $0.02m$. The difference between the offset was nearly completely eliminated. At the crossover a bigger distance offset can be noticed. This is caused by the intermediate values for which no LUT exist.

4 CONCLUSIONS

This article presents an easy but accurate data acquisition method for data evaluation of a customary sensor. Data evaluation focuses on the detection of the over- and underexposed data under consideration of objects with two different albedos. This improves the exactitude of the data for the study of the systematic errors of this sensor. Therefore the work of this article can be seen as an intermediate result on the way to a PMD range imaging sensor calibration. We showed that the object's reflectance properties affects the distance measuring. Therefore we proposed a basic method for the identification of the albedo of the considered objects so that an albedo according LUT can be applied for the correction. These LUT's have to be created for a set of reference objects with different albedos. The example in the previous section shows that a correction can be achieved about LUT's. Because of their contrariness in their albedos, we selected a white and a black wall as objects. A statement about the behaviour of the sensor can thereby be done only for those extreme albedos. Apart from these albedos a statement cannot occur for general reflectance properties. Further work has to be done in the field of interpolation between LUT's when unknown albedos are detected and how to handle crossovers between different albedo. Additionally, objects which reflectance properties cannot be described by a Lambertian reflectance model need to be investigated.

REFERENCES

Bouguet, J. (1999). *Visual methods for three-dimensional modeling*. PhD thesis, California Institute of Technology.

Kahlmann, T., Remondino, F., and Ingensand, H. (2006). Calibration for increased accuracy of the range imaging camera swissranger. In *International Archives of Photogrammetry, Remote Sensing and Spatial Information Sciences, ISPRS Commission V Symposium*, volume XXXVI, pages 136–141.

Lange, R. (2000). *3D Time-of-Flight Distance Measurement with Custom Solid-State Image Sensors in CMOS/CCD-Technology*. PhD thesis, University Siegen.

Lindner, M. and Kolb, A. (2006). Lateral and depth calibration of pmd-distance sensors. In *ISVC (2)- Advances in Visual Computing, Second International Symposium*, volume 4292 of *Lecture Notes in Computer Science*, pages 524–533. Springer Verlag.

Sabov, A. and Kruger, J. (2007). Improving the data quality of pmd-based 3d cameras. In *Proc. Vision, Modeling and Visualization (VMV)*.

Schwarte, R. (1999). *Handbook of Computer Vision and Applications*, chapter Principles of 3-D Imaging Techniques. Academic Press.